

# Crystalline Spectral Form Factors

Dmitrii A. Trunin<sup>1,\*</sup> and David A. Huse<sup>1</sup>

<sup>1</sup>*Department of Physics, Princeton University, Princeton, NJ 08544, USA*

(Dated: December 15, 2025)

We investigate crystalline-like behavior of the spectral form factor (SFF) in unitary quantum systems with extremely strong eigenvalue repulsion. Using a low-temperature Coulomb gas as a model of repulsive eigenvalues, we derive the Debye-Waller factor suppressing periodic oscillations of the SFF and estimate the order of its singularities at multiples of the Heisenberg time. We also reproduce this crystalline-like behavior using perturbed permutation circuits and random matrix ensembles associated with Lax matrices. Our results lay a foundation for future studies of quantum systems that exhibit intermediate level statistics between standard random matrix ensembles and permutation circuits.

**Introduction**— Spectral statistics and random matrix theory (RMT) are cornerstones of quantum chaos and quantum statistical mechanics [1–7]. Most quantum systems fall into one of the four major RMT classes [8] distinguished by the probability density function of eigenvalue (energy level) spacings  $s$ ,  $P(s) \sim s^\beta$  as  $s \rightarrow 0$ . Quantum chaos is associated with Wigner-Dyson statistics, which corresponds to  $\beta = 1, 2$  or  $4$  and implies level repulsion [9]. On the other hand, integrable systems lack level correlations and follow Poisson statistics with  $\beta = 0$  [10]. Since the inception of RMT in the framework of nuclear physics [11], these four universal classes have been observed in a wide range of quantum systems and provided essential tools for quantum many-body dynamics [12–16], quantum information theory [17], quantum optics [18], quantum transport [19], quantum gravity [20–25], and many other areas of physics.

However, some quantum systems fall outside the standard RMT classes with  $\beta = 0, 1, 2$  or  $4$ . One class of remarkable examples of non-conventional yet universal level statistics are provided by quantum cellular automata [26–35] and random permutation circuits [36–38]. In a properly chosen basis, discrete unitary time evolution of these models breaks down into large periodic cycles, so their quasi-energy spectrum reduces to sets of roots of unity [39]. Once the length of the largest cycle is comparable to the dimension of the Hilbert space (or dynamics is restricted to one of the invariant subspaces), quasi-energy levels become equally spaced on the unit circle. The probability density function of such a “picket fence” ensemble is exactly zero in the vicinity of level spacing  $s = 0$ , so this behavior corresponds to  $\beta = \infty$ . At the same time, these models are easily engineered and exhibit non-trivial dynamics. So, it becomes increasingly interesting to understand the emergence of quantum chaos in the entire range  $\beta \in (0, \infty)$ , and to find analytically tractable models that show behavior that interpolates between  $\beta = \infty$  and standard RMT classes.

In this Letter, we examine three models covering the lightly explored regime between  $\beta \sim 1$  and  $\beta = \infty$ : circular  $\beta$ -ensemble (Coulomb crystal of eigenvalues), perturbed permutation circuit, and random Lax matrix en-

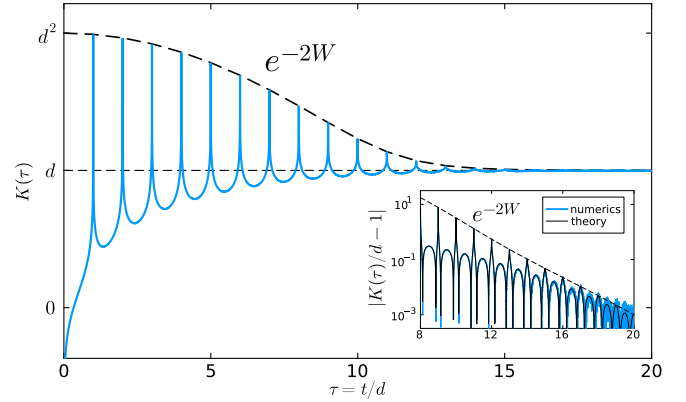


Figure 1. The SFF of the circular  $\beta$ -ensemble, which describes a Coulomb crystal of  $d = 512$  repulsive eigenvalues at inverse temperature  $\beta = 500$ . We average over  $10^6$  samples. Dashed line shows the damping Debye-Waller factor. Inset: deviation of the SFF from the plateau (zoom in the same graph).

semble. We study correlations between eigenvalues using the Fourier transform of the two-level distribution, also known as the spectral form factor (SFF):

$$K(t) = \left\langle |\text{Tr } U(t)|^2 \right\rangle = \sum_{m,n=0}^{d-1} \left\langle e^{i(E_m - E_n)t} \right\rangle. \quad (1)$$

Here,  $U(t) = (U(1))^t$  is the evolution operator for integer time  $t$ ,  $E_n$  are the corresponding (quasi)energies,  $d$  is the dimension of the Hilbert space, and  $\langle \dots \rangle$  is the ensemble average over statistically similar systems. Since the models that we study exhibit long-range (in energy) crystalline-like correlations of the eigenvalues of  $U = U(1)$ , we will employ the analogy with Bragg diffraction and treat the SFF as the structure factor of an eigenvalue crystal [40] which is subject to fluctuations. Following this analogy, quasi-energies  $E_m$  correspond to positions of atoms, and time  $t$  corresponds to the momentum change of the scattered wave.

The SFF is the simplest nontrivial quantity that captures eigenvalue correlations over the entire spectrum. In integrable systems the SFF decreases, in many cases

monotonically, from  $K(0) = d^2$  to  $K(t) \rightarrow d$  as  $t \rightarrow \infty$ . In conventionally quantum chaotic systems, it exhibits a telltale “dip—ramp—plateau” structure, which reflects level repulsion [4–6]. However, none of these standard SFF types show structure at long times  $t$  that are large multiples of  $d$ . The models that we study in this Letter all can exhibit crystalline-like oscillations of the SFF extending to  $t \gg d$  due to extremely strong level repulsion (Fig. 1). Similarly to Bragg diffraction from a real crystal, these oscillations are damped due to the weak fluctuations in the level patterns once we move away the exact  $\beta = \infty$  limit [40]. We calculate the damping Debye-Waller factor for all mentioned models and confirm it with numerical results. We also extend this calculation to higher-order derivatives in the case of the circular  $\beta$ -ensemble and show that well-known features of the SFF for the standard cases  $\beta = 1, 2, 4$  are remnants of Bragg peaks.

**Coulomb crystal of eigenvalues**— The circular  $\beta$ -ensemble extends the Wigner-Dyson level statistics of unitary operators from  $\beta = 1, 2, 4$  to an arbitrary real non-negative  $\beta$ . The joint probability distribution for the quasi-energies  $E_n$  of a unitary matrix drawn from the circular  $\beta$ -ensemble is described by the  $d$ -particle Coulomb gas confined to a unit circle at temperature  $T = 1/\beta$  [41]:

$$\begin{aligned} P(E_0, \dots, E_{d-1}) &= Z_{d,\beta}^{-1} e^{-\beta H(E_0, \dots, E_{d-1})}, \\ H(E_0, \dots, E_{d-1}) &= - \sum_{m < n} \log |e^{iE_m} - e^{iE_n}|, \end{aligned} \quad (2)$$

where  $Z_{d,\beta}$  is the normalizing factor (partition function).

We emphasize that, in general, the probability distribution of the random matrices that realize the circular  $\beta$ -ensemble is *not* invariant under basis transformations. Only the standard values  $\beta = 1, 2, 4$  correspond to basis-invariant ensembles [42]. Nonetheless, level statistics (2) with arbitrary  $\beta > 0$  does emerge in basis-specific settings, including a class of random-walk-like models [43–45]. This relationship allows us to sample the circular  $\beta$ -ensemble at low computational cost and study its spectral properties beyond  $\beta = 1, 2, 4$ . Furthermore, it opens a way for experimental tests and many-body generalizations of our models: see Supplemental Material and Ref. [46] for examples of quantum circuits implementing the circular  $\beta$ -ensemble.

To introduce the random-walk-like model of the circular  $\beta$ -ensemble, consider a quantum particle on a discrete interval with coordinates  $n = 0, 1, \dots, l-1$  and an additional internal degree of freedom with basis states  $|\pm\rangle$  (thus,  $d = 2l$ ). The discrete time evolution of the particle consists of alternating shift and scattering steps:

$$U = SLS^\dagger M. \quad (3)$$

The shift operator  $S$  is conditional: it always flips the particle but moves it only if it occupies the  $|+\rangle$  state:

$$S|n\rangle|-\rangle = S|n\rangle|+\rangle, \quad S|n\rangle|+\rangle = |n+1\rangle|-\rangle. \quad (4)$$

The scattering steps are described by  $2l \times 2l$  block-diagonal matrices commuting with the position operator:

$$L = \Theta_1 \oplus \Theta_3 \oplus \dots \oplus \Theta_{2l-1}, \quad M = \Theta_0 \oplus \Theta_2 \oplus \dots \oplus \Theta_{2l-2}, \quad (5)$$

where each  $2 \times 2$  block acts on the corresponding fixed-position subspace. Blocks  $n = 0, \dots, 2l-2$  are determined by complex numbers  $\alpha_n = e^{i\phi_n} \cos \theta_n$ , which control the mixing of  $|\pm\rangle$  states:

$$\Theta_n = \begin{pmatrix} e^{-i\phi_n} \cos \theta_n & \sin \theta_n \\ \sin \theta_n & -e^{i\phi_n} \cos \theta_n \end{pmatrix}. \quad (6)$$

We assume that these coefficients are independently distributed with the following probability density functions:

$$P(\alpha_n) \propto (1 - |\alpha_n|^2)^{(\beta(2l-1-n)/2)-1}. \quad (7)$$

The last block is diagonal and depends on a single real parameter uniformly distributed on the interval  $(-\pi, \pi)$ :  $\Theta_{2l-1} = e^{i\phi_{2l-1}} \oplus 1$ . This specifies the model: it is proven in [43, 44] that the eigenvalues of unitaries (3) are distributed according to the circular  $\beta$ -ensemble for any  $d = 2l$  (the model for an odd  $d$  is defined similarly).

**SFF of the Coulomb gas**— Before deriving the SFF of the circular  $\beta$ -ensemble for arbitrary  $\beta$ , let us first consider the low-temperature limit  $\beta \rightarrow \infty$ . In this limit, repulsion between Coulomb gas particles overcomes thermal fluctuations, but periodic boundary conditions keep particles confined. Hence, the gas condenses into a one-dimensional Coulomb crystal  $E_n = (2\pi n + \phi_{d-1})/d$ , where  $\phi_{d-1}$  is the overall phase (center of mass position). In this limit, the SFF becomes purely periodic in  $t$  with period  $d$ : For  $t = nd$  for  $n$  any integer  $K(t) = d^2$ . For all other (integer) values of  $t$ ,  $K(t) = 0$ . In terms of the random-walk-like model (3), the limit  $\beta \rightarrow \infty$  sets all coefficients  $\alpha_n$  to zero and turns scattering blocks into swap operators,  $\Theta_n \rightarrow \sigma_x$ . Hence, the evolution of the particle reduces to a cyclic permutation of basis states.

For a large but finite  $\beta$ , periodic oscillations of the SFF are suppressed at large  $t$  by thermal fluctuations. Assuming that these fluctuations are relatively small [47], we expand the Hamiltonian (2) near the saddle point,  $E_n = E_n^{(\beta=\infty)} + x_n$  with  $x_n \ll 2\pi/d$ , neglect higher-order nonlinear terms, and switch to the momentum picture:

$$H \approx \frac{1}{2} \sum_{p=1}^{d-1} p(d-p) \tilde{x}_p \tilde{x}_{-p}, \quad (8)$$

where  $\tilde{x}_p = \frac{1}{\sqrt{d}} \sum_{k=0}^{d-1} e^{-2\pi i k p/d} x_k$ . Note that the center-of-mass degree of freedom ( $p = 0$  mode) decouples, so we integrate it out. In this approximation, we explicitly estimate the ensemble average in the SFF (1):

$$\begin{aligned} K(t) &= \sum_{j,k} e^{2\pi i(k-j)t/d} \left\langle e^{it(x_k - x_j)} \right\rangle \\ &\approx d + d \sum_{k=1}^{d-1} e^{2\pi i k t/d} |Cd \sin(\pi k/d)|^{-4t^2/\beta d^2}. \end{aligned} \quad (9)$$

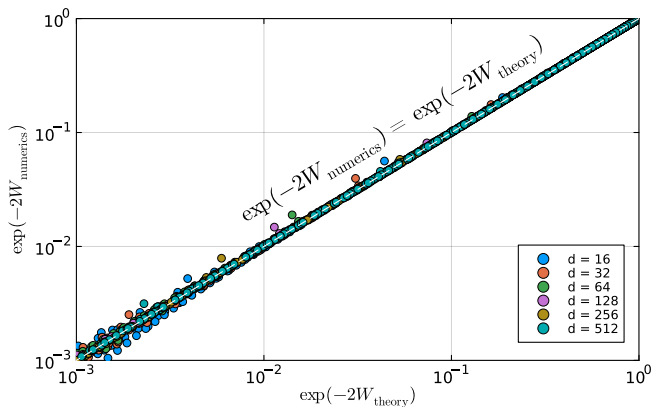


Figure 2. Comparison of numerical and theoretical Debye-Waller factors of the circular  $\beta$ -ensemble. Points for inverse temperatures  $1 < \beta < 20000$  are superposed.

We assume  $d \gg 1$  to approximate the sums involving two-point correlation functions. The numerical coefficient  $C \approx 3.6$ . Similarly to the zero-temperature SFF, “scattering amplitudes” constructively interfere near multiples of the Heisenberg time  $t_H = d$ . Hence, the finite-temperature SFF oscillates with period  $t_H$ . The effect of thermal vibrations is contained in the Debye-Waller factor  $e^{-2W}$ :

$$K(t_H\tau) \approx d + e^{-2W} d^2, \quad (10)$$

which suppresses peaks of the SFF ( $\tau = t/t_H = 1, 2, \dots$ ):

$$e^{-2W} \sim \begin{cases} d^{-4\tau^2/\beta}, & 4\tau^2/\beta \ll 1, \\ \log(d)/d, & 4\tau^2/\beta = 1, \\ (\beta/\tau^2 d)(C\pi)^{-4\tau^2/\beta}, & 4\tau^2/\beta \gg 1. \end{cases} \quad (11)$$

So, the peaks become negligible, and the SFF reaches the plateau only at times  $t \gg t_* \approx t_H \sqrt{\beta/4}$ . This new time scale is much larger than the Heisenberg time if  $\beta \gg 1$ .

The numerical calculations based on the random-walk-like model (3) agree well with theoretical estimates, e.g., see Figs. 1 and 2. In particular, we confirmed that full expression (9) and Debye-Waller factor (11) approximate the exact SFF with an error less than several per cent when  $\beta > 10$  and  $e^{-2W} > 0.01$ .

Furthermore, the Gaussian approximation captures the order of the SFF singularities at multiples of the Heisenberg time. Differentiating (9) by  $\tau = t/t_H$  in the limit  $d \rightarrow \infty$ , we find that the  $n$ -th derivative  $K^{(n)}(\tau)$  at  $\tau = 1, 2, \dots$  is divergent for  $n \geq \gamma$  (merely discontinuous if  $n = \gamma$  and  $n$  is odd), where

$$\gamma = 4\tau^2/\beta - 1. \quad (12)$$

In particular, this formula recovers the exact results [2] for  $\tau = 1$  ( $\beta = 1, 2, 4$ ) and  $\tau = 2$  ( $\beta = 4$ ). However, we emphasize that Gaussian approximation (9) works only

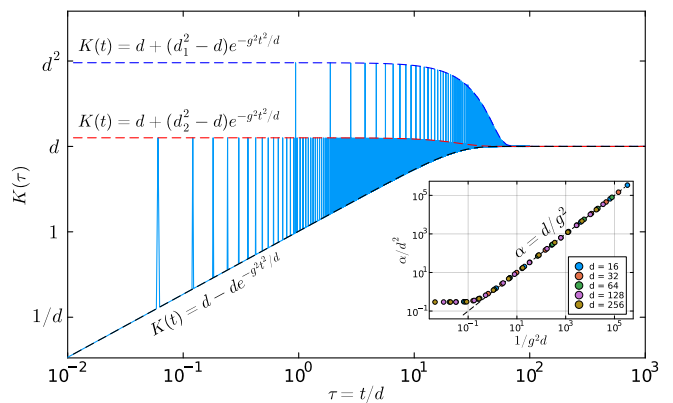


Figure 3. The SFF of toy model (13) interpolating between  $\beta = 2$  and  $\beta = \infty$ . We set  $d = 512$ ,  $g = 0.002$ , and average over  $10^5$  samples. The base permutation  $S$  contains two cycles of length  $d_1 = 481$  and  $d_2 = 31$ . Inset: The strength of the pinning potential  $V(x) = \alpha x^2/2$  determined by fitting the SFF with Eq. (14). The permutation used in the inset contains a single cycle.

for relatively small times  $\tau \ll \beta$  (see Supplemental Material for details). This limitation explains the discrepancy between Eq. (12) and exact  $\beta = 1, 2, 4$  results at larger times, where the SFF in those specific cases has no singularities. Nevertheless, it leaves ample room for conspicuous crystalline-like behavior of the SFF when  $\beta \gg 1$ .

**Perturbed permutation circuit**— There are other models interpolating between the standard RMT universality classes. Besides empirical Brody [48, 49] and Berry-Robnik [50] distributions, explicit examples of intermediate level statistics include banded matrices [51–54], Pandey-Mehta [55–58], Rosenzweig-Porter [59, 60], and other toy models [61–69]. However, these models are restricted to the interval between  $\beta = 0$  and  $\beta = 2$ . Hence, they cannot produce the crystalline-like behavior of the SFF that is present at large  $\beta$ . We suggest a new simple model, which interpolates between  $\beta = 2$  and  $\beta = \infty$ :

$$U = \exp(-igH) S. \quad (13)$$

Here,  $H$  is a random  $d \times d$  Hermitian matrix drawn from the Gaussian Unitary Ensemble (GUE) with probability density  $\propto \exp[-(d/2)\text{Tr}HH^\dagger]$ ,  $S$  is a classical permutation of basis vectors supplemented with independent and uniformly distributed random phase rotations,  $S|k\rangle = e^{i\phi_k} |\pi(k)\rangle$ , and  $0 \leq g \leq \pi/2$  is a real parameter controlling the strength of this GUE perturbation to the permutation. For simplicity, we consider global matrices  $H$  and  $S$ ; however, model (13) is straightforwardly reproduced by a local shallow circuit [70]. We also assume that the permutation  $\pi(k)$  is fixed but drawn at random. In this case, the typical length of its largest cycle is comparable to  $d$  [71], and the Heisenberg time  $t_H = \mathcal{O}(d)$ .

Similarly to the circular  $\beta$ -ensemble, we first consider the limit  $g \rightarrow 0$ . In this limit, eigenvalues of unitary (13)

weakly fluctuate near the eigenvalues of the permutation matrix  $S$ , so we can use perturbation theory to evaluate the SFF. In general, permutation  $\pi(k)$  contains  $N$  cycles of length  $d_n$ , and each cycle produces a series of equally-spaced SFF peaks:

$$K(t) \approx d + e^{-t^2 g^2/d} \left[ \left( \sum_{n=1}^N d_n \delta_{t \bmod d_n, 0} \right)^2 - d \right]. \quad (14)$$

In other words, the model describes  $N$  independent crystals of  $d_n$  non-interacting particles (eigenvalues) pinned to the corresponding lattices by a harmonic potential  $V(x) = \alpha x^2/2$  with  $\alpha = d/g^2$ , with temperature one.

For small but finite  $g \ll 1/\sqrt{d}$ , eigenvalue fluctuations are smaller than level spacings, so the structure of the SFF (14) and the damping Debye-Waller factors are qualitatively preserved, see Fig. 3. In this limit, the SFF reaches the plateau for  $t \gg t_* \sim \sqrt{d} \log d/g \gg t_H$ . In the opposite limit  $d \gg 1/g^2$ , repulsion between eigenvalues recovers the circular unitary ensemble (CUE), so the SFF approaches the standard “dip—ramp—plateau” form after the Thouless time  $t_{\text{Th}} \sim \sqrt{d}/g \ll t_H$ . Thus as  $dg^2$  is varied, this system interpolates between a perfect crystal that matches  $\beta \rightarrow \infty$  and the  $\beta = 2$  CUE, but in between these two limits its SFF is different from the intermediate circular  $\beta$ -ensembles.

**Random Lax matrix ensemble**— The last example of the crystalline SFF is given by the ensemble of random Lax matrices  $U$  of the Ruijsenaars-Schneider model [72, 73], which also emerges as quantization of interval-exchange maps [74, 75]:

$$U_{mn} = \frac{1}{d} e^{ip_m} \frac{1 - e^{2\pi i g}}{1 - e^{2\pi i(m-n+g)/d}}, \quad (15)$$

where  $p_m$  are independent random variables uniformly distributed between  $-\pi$  and  $\pi$ ,  $d$  is the dimension of the Hilbert space, and parameter  $0 < g < 1$  controls level repulsion. In the limit  $g \rightarrow 0$ , unitary (15) becomes diagonal and has Poisson level statistics. In the limit  $g \rightarrow 1$ , it turns into a cyclic shift operator supplemented with random phase rotations:  $U_{mn} = e^{ip_m} \delta_{m+1,n}$ , so has a zero-temperature eigenvalue crystal. Thus these two limits correspond to  $\beta = 0$  and  $\beta = \infty$ , respectively. For intermediate values of  $g$ , the spectral statistics of  $U$  is described by a gas of hard rods [73]:

$$P(E_0, \dots, E_{d-1}) \propto \prod_{j=0}^{d-1} \theta \left( E_{j+1} - E_j - \frac{2\pi}{d} g \right), \quad (16)$$

where  $g$  is the scaled length of the rods, and  $E_j$  are the positions of the rod centers. Thus this system provides an interpolation between  $\beta = 0$  and  $\beta = \infty$ ; again, between these two limits this system differs from the circular  $\beta$ -ensembles. For large  $d$ , the SFF behaves as:

$$\frac{K(t = \tau d)}{d} \approx 1 + 2\text{Re} \frac{1}{e^{2\pi i g \tau} [1 + 2\pi i(1-g)\tau] - 1}. \quad (17)$$

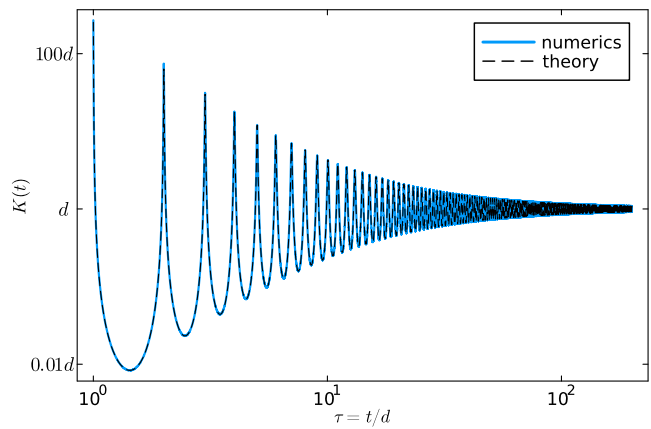


Figure 4. SFF of the random ensemble of Lax matrices (15). We set  $d = 512$ ,  $g = 0.98$ , and average over  $10^5$  samples.

This result is exact in the limit  $d \rightarrow \infty$  [73] and agrees with numerical results for  $d \gg 1$ , e.g., see Fig. 4. Similarly to the SFF of the Coulomb gas (9), this SFF oscillates in an earlier time regime with period  $t_H \approx d$  when  $1 - g \ll 1$ . Not so similarly,  $K(t)/d$  and all of its time derivatives remain finite for  $0 < g < 1$  and any  $\tau = t/d > 0$  in the limit  $d \rightarrow \infty$ . For  $0 < t \ll d/(1-g)$  the peaks in  $K(t)/d$  are of height  $\sim [d/((1-g)t)]^2 \gg 1$  and thus strong. For later times,  $K(t)/d$  continues to weakly oscillate, but now with a longer period  $d/g$  and amplitude  $\sim d/((1-g)t) \ll 1$ .

**Conclusion**— We have presented three models of “crystalline” level statistics associated with oscillations of the SFF. For all three models, we have analytically derived expressions for the Debye-Waller factor, which suppresses oscillations of the SFF, and the new time scale  $t_* \gg t_H$ , at which the SFF approaches the plateau. The key ingredient ensuring such a crystalline-like behavior is the strong level repulsion. Our examples indicate that this behavior occurs in some broader class of chaotic quantum systems. We also emphasize that this class is not restricted to unitary discrete-time evolution, although the examples we gave are of this type. In particular, the necessary requirement for crystalline level statistics is satisfied by the Gaussian  $\beta$ -ensemble at large  $\beta$  [76], the weakly-disordered one-dimensional Anderson localization model [77], an ensemble of random Lax matrices of Calogero-Moser model [72, 73], and inhomogeneous discrete-time quantum walks [78–86].

We expect that our work paves a way for further investigations in various directions. First, crystalline-like eigenvalue statistics implies that dephasing in the eigenstate basis is delayed until time  $t_* \gg t_H$ , so it suggests a careful study of the behavior of correlation functions, entanglement, complexity, and other essential tools of quantum dynamics, for our examples between  $t_H$  and  $t_*$ . Second, it would be interesting to find and investigate many-

body systems with crystalline-like level statistics intermediate between  $\beta \sim 1$  and  $\beta = \infty$ . A straightforward generalization of the discrete-walk-like model (3) to the case of free non-interacting fermions, which we describe in the Supplemental Material, resembles other toy models of the many-body SFF [87–90] and serves as a good starting point for this endeavor. Besides, models of intermediate level statistics between  $\beta = 0$  and  $\beta \sim 1$  play an important role for the studies of many-body-localization transitions [91–94]. It would be thrilling to find an analog of this transition between  $\beta \sim 1$  and  $\beta = \infty$ . Finally, recent experimental advancements [95] make it tempting to experimentally confirm the crystalline-like behavior of the SFF in our models.

**Acknowledgements**— The authors thank Sarang Gopalakrishnan and Amit Vikram for helpful discussions. D.A.H. was supported in part by NSF QLCI grant OMA-2120757.

---

\* dmitrii.trunin@princeton.edu

- [1] C. E. Porter, *Statistical Theories of Spectra: Fluctuations*, Perspectives in Physics (Academic Press, New York, NY, 1965).
- [2] M. L. Mehta, *Random Matrices*, Pure and Applied Mathematics, Vol. 142 (Elsevier, New York, 2004).
- [3] P. J. Forrester, *Log-Gases and Random Matrices*, London Mathematical Society Monographs, Vol. 34 (Princeton University Press, Princeton, NJ, 2010).
- [4] F. Haake, *Quantum Signatures of Chaos* (Springer-Verlag Berlin Heidelberg, 2010).
- [5] H.-J. Stöckmann, *Quantum Chaos: An Introduction* (Cambridge University Press, Cambridge, England, 1999).
- [6] T. Guhr, A. Müller-Groeling, and H. A. Weidenmüller, Random matrix theories in quantum physics: Common concepts, *Phys. Rept.* **299**, 189 (1998), arXiv:cond-mat/9707301.
- [7] L. D’Alessio, Y. Kafri, A. Polkovnikov, and M. Rigol, From quantum chaos and eigenstate thermalization to statistical mechanics and thermodynamics, *Adv. Phys.* **65**, 239 (2016), arXiv:1509.06411.
- [8] A complete classification of random matrix ensembles reveals additional spectral features [? ? ].
- [9] O. Bohigas, M. J. Giannoni, and C. Schmit, Characterization of chaotic quantum spectra and universality of level fluctuation laws, *Phys. Rev. Lett.* **52**, 1 (1984).
- [10] M. V. Berry and M. Tabor, Level clustering in the regular spectrum, *Proc. R. Soc. Lond. A* **356**, 375 (1977).
- [11] H. A. Weidenmüller and G. E. Mitchell, Random matrices and chaos in nuclear physics. Part 1. nuclear structure, *Rev. Mod. Phys.* **81**, 539 (2009), arXiv:0807.1070.
- [12] M. Srednicki, Chaos and quantum thermalization, *Phys. Rev. E* **50**, 888 (1994), arXiv:cond-mat/9403051.
- [13] M. Rigol, V. Dunjko, and M. Olshanii, Thermalization and its mechanism for generic isolated quantum systems, *Nature* **452**, 854 (2008), arXiv:0708.1324.
- [14] S. Sachdev, *Quantum Phase Transitions*, Lecture Notes in Physics Monographs (Vol. 18) (Cambridge University Press, Cambridge, England, 2011).
- [15] R. Nandkishore and D. A. Huse, Many body localization and thermalization in quantum statistical mechanics, *Ann. Rev. Condensed Matter Phys.* **6**, 15 (2015), arXiv:1404.0686.
- [16] D. A. Abanin, E. Altman, I. Bloch, and M. Serbyn, Colloquium: Many-body localization, thermalization, and entanglement, *Rev. Mod. Phys.* **91**, 021001 (2019), arXiv:1804.11065.
- [17] B. Collins and I. Nechita, Random matrix techniques in quantum information theory, *J. Math. Phys.* **57**, 015215 (2016), arXiv:1509.04689.
- [18] H. Carmichael, *An Open Systems Approach to Quantum Optics*, Lecture Notes in Physics Monographs (Vol. 18) (Springer-Verlag Berlin Heidelberg, 1993).
- [19] C. W. J. Beenakker, Random-matrix theory of quantum transport, *Rev. Mod. Phys.* **69**, 731 (1997), arXiv:cond-mat/9612179.
- [20] E. Brézin, C. Itzykson, G. Parisi, and J. B. Zuber, Planar diagrams, *Commun. Math. Phys.* **59**, 35 (1978).
- [21] J. S. Cotler, G. Gur-Ari, M. Hanada, J. Polchinski, P. Saad, S. H. Shenker, D. Stanford, A. Streicher, and M. Tezuka, Black holes and random matrices, *J. High Energy Phys.* **2017** (05), 118, [Erratum: J. High Energy Phys. **2022** (09), 002], arXiv:1611.04650.
- [22] P. Saad, S. H. Shenker, and D. Stanford, JT gravity as a matrix integral, arXiv:1903.11115.
- [23] J. Cotler and K. Jensen, AdS<sub>3</sub> gravity and random CFT, *J. High Energy Phys.* **2021** (04), 033, arXiv:2006.08648.
- [24] A. Belin, J. de Boer, D. L. Jafferis, P. Nayak, and J. Sonner, Approximate CFTs and random tensor models, *J. High Energy Phys.* **2024** (09), 163, arXiv:2308.03829.
- [25] D. L. Jafferis, L. Rozenberg, and G. Wong, 3d gravity as a random ensemble, *J. High Energy Phys.* **2025** (02), 208, arXiv:2407.02649.
- [26] T. Farrelly, A review of quantum cellular automata, *Quantum* **4**, 368 (2020), arXiv:1904.13318.
- [27] P. Arrighi, An overview of quantum cellular automata, *Natural Comput.* **18**, 885 (2019), arXiv:1904.12956.
- [28] S. Gopalakrishnan and B. Zakirov, Facilitated quantum cellular automata as simple models with nonthermal eigenstates and dynamics, *Quantum Sci. Technol.* **3**, 044004 (2018), arXiv:1802.07729.
- [29] S. Gopalakrishnan, Operator growth and eigenstate entanglement in an interacting integrable Floquet system, *Phys. Rev. B* **98**, 060302 (2018), arXiv:1806.04156.
- [30] S. Gopalakrishnan, D. A. Huse, V. Khemani, and R. Vasseur, Hydrodynamics of operator spreading and quasiparticle diffusion in interacting integrable systems, *Phys. Rev. B* **98**, 220303 (2018), arXiv:1809.02126.
- [31] V. Alba, J. Dubail, and M. Medenjak, Operator entanglement in interacting integrable quantum systems: The case of the rule 54 chain, *Phys. Rev. Lett.* **122**, 250603 (2019), arXiv:1901.04521.
- [32] J. Iaconis, S. Vijay, and R. Nandkishore, Anomalous subdiffusion from subsystem symmetries, *Phys. Rev. B* **100**, 214301 (2019), arXiv:1907.10629.
- [33] J. Iaconis, A. Lucas, and R. Nandkishore, Multipole conservation laws and subdiffusion in any dimension, *Phys. Rev. E* **103**, 022142 (2021), arXiv:2009.06507.
- [34] J. Feldmeier, P. Sala, G. de Tomasi, F. Pollmann, and M. Knap, Anomalous diffusion in dipole- and higher-moment conserving systems, *Phys. Rev. Lett.* **125**, 245303 (2020), arXiv:2004.00635.

- [35] L. E. Hillberry, L. Piroli, E. Vernier, N. Y. Halpern, T. Prosen, and L. D. Carr, Integrability of Goldilocks quantum cellular automata, [arXiv:2404.02994](#).
- [36] B. Bertini, K. Klobas, P. Kos, and D. Malz, Quantum and classical dynamics with random permutation circuits, *Phys. Rev. X* **15**, 011015 (2025), [arXiv:2407.11960](#).
- [37] D. Szász-Schagrin, M. Mazzoni, B. Bertini, K. Klobas, and L. Piroli, Entanglement dynamics and Page curves in random permutation circuits, [arXiv:2505.06158](#).
- [38] B. Bertini, K. Klobas, P. Kos, and D. Malz, Random permutation circuits are quantum chaotic, [arXiv:2508.10890](#).
- [39] Possibly shifted by a constant phase.
- [40] N. W. Ashcroft and N. D. Mermin, *Solid State Physics* (Holt, Rinehart and Winston, New York, 1976).
- [41] The equilibration of the Coulomb gas is described by the Dyson Brownian motion [1–3] and reproduces probability distribution (2). We emphasize that this description does not rely on the specific properties of  $\beta = 1, 2, 4$ .
- [42] Physically sound basis transformations are described by an associative division algebra over real numbers. According to the Frobenius theorem, all such algebras are isomorphic to either real, complex, or quaternion numbers. These algebras correspond to the orthogonal ( $\beta = 1$ ), unitary ( $\beta = 2$ ), and symplectic ( $\beta = 4$ ) basis transformations, respectively.
- [43] R. Killip and I. Nenciu, Matrix models for circular ensembles, *Int. Math. Res. Not.* **2004**, 2665 (2004), [arXiv:math/0410034](#).
- [44] R. Killip and M. Stoiciu, Eigenvalue statistics for CMV matrices: From Poisson to clock via random matrix ensembles, *Duke Math. J.* **146**, 361 (2009), [arXiv:math-ph/0608002](#).
- [45] M. J. Cantero, L. Moral, and L. Velazquez, Five-diagonal matrices and zeros of orthogonal polynomials on the unit circle, *Linear Algebra Appl.* **362**, 29 (2003), [arXiv:math/0204300](#).
- [46] N. Kolganov and D. A. Trunin, Streamlined Krylov construction and classification of ergodic Floquet systems, *Phys. Rev. E* **111**, L052202 (2025), [arXiv:2412.19797](#).
- [47] Expansion near infinite-temperature eigenvalues is self-consistent if the fluctuation amplitude is smaller than average level spacing, i.e.,  $\Delta x_k^2 \approx 2 \log d / \beta d^2 < (2\pi/d)^2$ . Hence, it is justified for  $\beta > 1$  and any numerically feasible system size ( $d < 10^8$ ).
- [48] T. A. Brody, A statistical measure for the repulsion of energy levels, *Lett. Nuovo Cimento* **7**, 482 (1973).
- [49] T. A. Brody, J. Flores, J. B. French, P. A. Mello, A. Pandey, and S. S. M. Wong, Random-matrix physics: spectrum and strength fluctuations, *Rev. Mod. Phys.* **53**, 385 (1981).
- [50] M. V. Berry and M. Robnik, Semiclassical level spacings when regular and chaotic orbits coexist, *J. Phys. A: Math. Gen.* **17**, 2413 (1984).
- [51] M. Moshe, H. Neuberger, and B. Shapiro, A generalized ensemble of random matrices, *Phys. Rev. Lett.* **73**, 1497 (1994), [arXiv:cond-mat/9403085](#).
- [52] A. D. Mirlin, Y. V. Fyodorov, F.-M. Dittes, J. Quezada, and T. H. Seligman, Transition from localized to extended eigenstates in the ensemble of power-law random banded matrices, *Phys. Rev. E* **54**, 3221 (1996), [arXiv:cond-mat/9604163](#).
- [53] E. Bogomolny and O. Giraud, Eigenfunction entropy and spectral compressibility for critical random matrix ensembles, *Phys. Rev. Lett.* **106**, 044101 (2011), [arXiv:1011.3686](#).
- [54] F. Evers and A. D. Mirlin, Anderson transitions, *Rev. Mod. Phys.* **80**, 1355 (2008), [arXiv:0707.4378](#).
- [55] A. Pandey and M. L. Mehta, Gaussian ensembles of random Hermitian matrices intermediate between orthogonal and unitary ones, *Commun. Math. Phys.* **87**, 449 (1983).
- [56] G. Lenz and F. Haake, Transitions between universality classes of random matrices, *Phys. Rev. Lett.* **65**, 2325 (1990).
- [57] G. Lenz and F. Haake, Reliability of small matrices for large spectra with nonuniversal fluctuations, *Phys. Rev. Lett.* **67**, 1 (1991).
- [58] N. Dupuis and G. Montambaux, Aharonov-Bohm flux and statistics of energy levels in metals, *Phys. Rev. B* **43**, 14390 (1991).
- [59] N. Rosenzweig and C. E. Porter, “Repulsion of energy levels” in complex atomic spectra, *Phys. Rev.* **120**, 1698 (1960).
- [60] V. E. Kravtsov, I. M. Khaymovich, E. Cuevas, and M. Amini, A random matrix model with localization and ergodic transitions, *New J. Phys.* **17**, 122002 (2015), [arXiv:1508.01714](#).
- [61] F. M. Izrailev, Simple models of quantum chaos: Spectrum and eigenfunctions, *Phys. Rept.* **196**, 299 (1990).
- [62] T. Prosen and M. Robnik, Energy level statistics in the transition region between integrability and chaos, *J. Phys. A: Math. Gen.* **26**, 2371 (1993).
- [63] T. Prosen and M. Robnik, Semiclassical energy level statistics in the transition region between integrability and chaos: transition from Brody-like to Berry-Robnik behaviour, *J. Phys. A: Math. Gen.* **27**, 8059 (1994).
- [64] T. Prosen, Time evolution of a quantum many-body system: transition from integrability to ergodicity in thermodynamic limit, *Phys. Rev. Lett.* **80**, 1808 (1998), [arXiv:cond-mat/9707180](#).
- [65] T. Prosen, On general relation between quantum ergodicity and fidelity of quantum dynamics, *Phys. Rev. E* **65**, 036208 (2002), [arXiv:quant-ph/0106149](#).
- [66] B. Bertini, P. Kos, and T. Prosen, Exact spectral form factor in a minimal model of many-body quantum chaos, *Phys. Rev. Lett.* **121**, 264101 (2018), [arXiv:1805.00931](#).
- [67] A. Chan, A. De Luca, and J. T. Chalker, Spectral statistics in spatially extended chaotic quantum many-body systems, *Phys. Rev. Lett.* **121**, 060601 (2018), [arXiv:1803.03841](#).
- [68] A. J. Friedman, A. Chan, A. De Luca, and J. T. Chalker, Spectral statistics and many-body quantum chaos with conserved charge, *Phys. Rev. Lett.* **123**, 210603 (2019), [arXiv:1906.07736](#).
- [69] P. Sierant and J. Zakrzewski, Model of level statistics for disordered interacting quantum many-body systems, *Phys. Rev. B* **101**, 104201 (2020), [arXiv:1907.10336](#).
- [70] We discuss a straightforward local generalization of model (13) in the Supplemental Material. Besides, local permutation circuits with exponentially large cycles can be constructed using primitive polynomials over the binary field, e.g., see [? ?].
- [71] K. Ford, Cycle type of random permutations: A toolkit, *Discrete Analysis* **2022**, 36 (2022), [arXiv:2104.12019](#).
- [72] E. Bogomolny, O. Giraud, and C. Schmit, Random matrix ensembles associated with Lax matrices, *Phys. Rev. Lett.* **103**, 054103 (2009), [arXiv:0904.4898](#).

- [73] E. Bogomolny, O. Giraud, and C. Schmit, Integrable random matrix ensembles, *Nonlinearity* **24**, 3179 (2011), [arXiv:1104.3777](#).
- [74] E. Bogomolny and C. Schmit, Spectral statistics of a quantum interval-exchange map, *Phys. Rev. Lett.* **93**, 254102 (2004), [arXiv:nlin/0408062](#).
- [75] O. Giraud, J. Marklof, and S. O'Keefe, Intermediate statistics in quantum maps, *J. Phys. A: Math. Gen.* **37**, L303 (2004), [arXiv:nlin/0403033](#).
- [76] I. Dumitriu and A. Edelman, Matrix models for beta ensembles, *J. Math. Phys.* **43**, 5830 (2002), [arXiv:math-ph/0206043](#).
- [77] E. Jonathan Torres-Herrera, J. A. Méndez-Bermúdez, and L. F. Santos, Level repulsion and dynamics in the finite one-dimensional Anderson model, *Phys. Rev. E* **100**, 022142 (2019), [arXiv:1904.11989](#).
- [78] M. J. Cantero, F. A. Grünbaum, L. Moral, and L. Velazquez, Matrix valued Szegő polynomials and quantum random walks, *Commun. Pure Appl. Math.* **63**, 464 (2010), [arXiv:0901.2244](#).
- [79] N. Linden and J. Sharam, Inhomogeneous quantum walks, *Phys. Rev. A* **80**, 052327 (2009), [arXiv:0906.3692](#).
- [80] C. V. Ambarish, N. Lo Gullo, T. Busch, L. Dell'Anna, and C. Chandrashekar, Dynamics and energy spectra of aperiodic discrete-time quantum walks, *Phys. Rev. E* **96**, 012111 (2017), [arXiv:1611.04427](#).
- [81] L. Gong, J. Sun, X. Guo, W. Cheng, and S. Zhao, Statistics of Floquet quasienergy spectrum for one-dimensional periodic, Fibonacci quasiperiodic and random discrete-time quantum walks, *Eur. Phys. J. B* **95**, 78 (2022).
- [82] J. Kempe, Quantum random walks: An introductory overview, *Contemp. Phys.* **44**, 307 (2003), [arXiv:quant-ph/0303081](#).
- [83] S. E. Venegas-Andraca, Quantum walks: A comprehensive review, *Quant. Inf. Proc.* **11**, 1015 (2012), [arXiv:1201.4780](#).
- [84] Y. Aharonov, L. Davidovich, and N. Zagury, Quantum random walks, *Phys. Rev. A* **48**, 1687 (1993).
- [85] A. Ambainis, E. Bach, A. Nayak, A. Vishwanath, and J. Watrous, One-dimensional quantum walks, in *Proceedings of the Thirty-Third Annual ACM Symposium on Theory of Computing*, STOC '01 (Association for Computing Machinery, New York, NY, 2001) p. 37.
- [86] C. Ryan, M. Laforest, J. Boileau, and R. Laflamme, Experimental implementation of a discrete-time quantum random walk on an NMR quantum-information processor, *Phys. Rev. A* **72**, 062317 (2005), [arXiv:quant-ph/0507267](#).
- [87] Y. Liao, A. Vikram, and V. Galitski, Many-body level statistics of single-particle quantum chaos, *Phys. Rev. Lett.* **125**, 250601 (2020), [arXiv:2005.08991](#).
- [88] M. Winer, S.-K. Jian, and B. Swingle, An exponential ramp in the quadratic Sachdev-Ye-Kitaev model, *Phys. Rev. Lett.* **125**, 250602 (2020), [arXiv:2006.15152](#).
- [89] M. O. Flynn, L. Vidmar, and T. N. Ikeda, Single-particle universality of the many-body spectral form factor, *Phys. Rev. Lett.* **134**, 160403 (2025), [arXiv:2410.07306](#).
- [90] T. N. Ikeda, L. Vidmar, and M. O. Flynn, Exact spectral form factors of noninteracting fermions with Dyson statistics, *Phys. Rev. B* **111**, 144312 (2025), [arXiv:2410.08269](#).
- [91] V. Oganessian and D. A. Huse, Localization of interacting fermions at high temperature, *Phys. Rev. B* **75**, 155111 (2007), [arXiv:cond-mat/0610854](#).
- [92] Y. Y. Atas, E. Bogomolny, O. Giraud, and G. Roux, Distribution of the ratio of consecutive level spacings in random matrix ensembles, *Phys. Rev. Lett.* **110**, 084101 (2013), [arXiv:1212.5611](#).
- [93] W. Buijsman, V. Cheianov, and V. Gritsev, Random matrix ensemble for the level statistics of many-body localization, *Phys. Rev. Lett.* **122**, 180601 (2019), [arXiv:1807.05075](#).
- [94] A. Prakash, J. H. Pixley, and M. Kulkarni, Universal spectral form factor for many-body localization, *Phys. Rev. Res.* **3**, L012019 (2021), [arXiv:2008.07547](#).
- [95] H. Dong *et al.*, Measuring the spectral form factor in many-body chaotic and localized phases of quantum processors, *Phys. Rev. Lett.* **134**, 010402 (2025), [arXiv:2403.16935](#).

# Supplemental Material for “Crystalline Spectral Form Factors”

Here, we report some useful information supplementing the main text. In particular:

- In Sec. I, we introduce quantum circuit models of the one-dimensional Coulomb gas (circular  $\beta$ -ensemble);
- In Sec. II, we discuss the limitations of the Gaussian approximation for the SFF of the circular  $\beta$ -ensemble;
- in Sec. III, we derive the Debye-Waller factor of the toy interpolating model  $U = e^{-igH}S$ ;
- in Sec. IV, we describe a local shallow circuit that reproduces the toy interpolating model  $U = e^{-igH}S$ .

## I. QUANTUM CIRCUITS FOR THE CIRCULAR BETA ENSEMBLE

There are two simple ways to implement the random-walk-like model  $U = SLS^\dagger M$  using a quantum circuit. In the first approach, we simply identify the basis of the hopping particle with computational basis states of an  $N$ -qubit quantum circuit:

$$|n\rangle|\pm\rangle \rightarrow |2n + (1 \pm 1)/2\rangle = |2^{N-1}b_{N-1} + \dots + 2b_1 + b_0\rangle = \bigotimes_{k=0}^{N-1} |b_k\rangle, \quad (1)$$

where  $b_k = 0, 1$ . In this basis, matrix  $S$  merely represents a cyclic adding operation,  $S|n\rangle = |n+1\rangle$ , and block-diagonal matrices  $L$  and  $M$  are nothing but quantum multiplexers, i.e., multi-qubit controlled operations. In other words, they conditionally apply the gate  $\Theta_{2k+\lambda}$  to the target 0-th qubit, where  $k = 2^{N-2}b_{N-1} + \dots + 2b_2 + b_1$  is determined by the state of control qubits  $|b_{N-1}\rangle \otimes \dots \otimes |b_1\rangle$  and  $\lambda = 0, 1$  for operators  $M, L$ , respectively. Note that in general,  $2^N \geq d$ , where  $d = 2l$  is the dimension of the original Hilbert space of the hopping particle; if equality does not hold, we simply set  $\Theta_k = \mathbb{I}$  for  $k > d$ . This circuit is depicted on Fig. 1(a).

The second approach that implements  $U$  in quantum circuits promotes the one-particle random walk to a many-particle one. Namely, we construct the following two-layer brick-work circuit acting on  $2l$  qubits (we identify qubits  $2l$  and 0):

$$U = \prod_{k=0}^{l-1} \tilde{\Theta}_{2k+1}(2k+1, 2k+2) \prod_{k=0}^{l-1} \tilde{\Theta}_{2k}(2k, 2k+1). \quad (2)$$

In this notation, two-qubit gates  $\tilde{\Theta}_k(m, n)$ , which act on qubits  $m$  and  $n$ , are constructed from the same single-qubit blocks  $\Theta_k$  as matrices  $L$  and  $M$ :

$$\tilde{\Theta}_k(m, n) = \text{CNOT}(n \rightarrow m)\Theta_k(m \rightarrow n)\text{CNOT}(n \rightarrow m) = \begin{pmatrix} 1 & 0 & 0 & 0 \\ 0 & e^{-i\phi_k} \cos \theta_k & \sin \theta_k & 0 \\ 0 & \sin \theta_k & -e^{i\phi_k} \cos \theta_k & 0 \\ 0 & 0 & 0 & 1 \end{pmatrix}, \quad (3)$$

where  $O(c \rightarrow t)$  denotes a controlled- $O$  gate with controlled qubit  $c$  and target qubit  $t$ . Circuit  $U$  clearly preserves the number of particles  $Q = \sum_k b_k$  and reproduces the one-particle hopping problem in the subspace  $Q = 1$ . This circuit is depicted on Fig. 1(b).

## II. LIMITS OF THE GAUSSIAN APPROXIMATION

In this section, we explain why Gaussian approximation for the SFF of the circular  $\beta$ -ensemble fails at times  $t/d \gg \beta$ . To that end, we again expand the Hamiltonian of the circular  $\beta$ -ensemble near the zero-temperature equilibrium positions,  $E_n = E_n^{\beta=\infty} + x_n$ , but keep the first non-linear term:

$$H = \frac{1}{2}d^2 \sum_{p=1}^{d-1} S_2\left(\frac{p}{d}\right) \tilde{x}_p \tilde{x}_{-p} + id^{5/2} \sum_{p,q=1}^{d-1} S_3\left(\frac{p+q}{d}\right) \tilde{x}_p \tilde{x}_q \tilde{x}_{-p-q} + \dots, \quad (4)$$

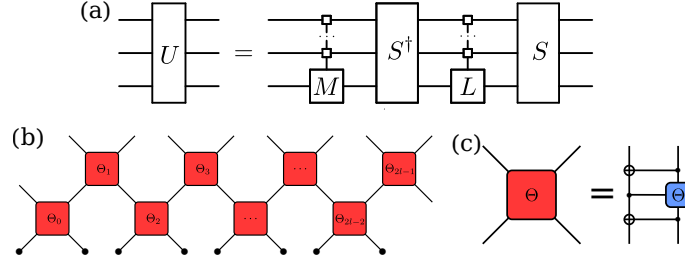


Figure 1. Quantum circuits implementing the random-walk-like model of the circular  $\beta$ -ensemble. (a) One-particle model on  $N$  qubits ( $2^N \geq d$ ). (b) Many-body model on  $d$  qubits, which describes non-interacting fermions and reproduces the original model in the one-particle sector. (c) Structure of the two-qubit gates comprising the brick-work circuit (b).

where we introduced the following short notations:

$$S_2(x) = x(1-x), \quad S_3(x) = \frac{1}{d^3} \sum_{k=1}^d \frac{\cos(\pi k/d)}{4 \sin^3(\pi k/d)} \sin(2\pi kx). \quad (5)$$

Then we rewrite the SFF in terms of Fourier harmonics  $\tilde{x}_p$ :

$$K(t) = \sum_{j,k} e^{2\pi i(j-k)/d} \left\langle e^{it(x_j - x_k)} \right\rangle = \sum_{j,k} e^{2\pi i(j-k)/d} \left\langle e^{it \sum_p S_{j,k}(p) \tilde{x}_p} \right\rangle, \quad S_{j,k}(p) = \frac{1}{\sqrt{d}} \left( e^{2\pi ijp/d} - e^{2\pi ikp/d} \right). \quad (6)$$

Thus, we need to estimate the expectation value  $V = \left\langle \exp \left[ it \sum_p S_{j,k}(p) \tilde{x}_p \right] \right\rangle$  in the theory (4). We know that  $S_2, S_3 \sim 1$  and that on average, the deviation of modes  $\langle \tilde{x}_p^2 \rangle \sim \log(d)/\beta d^2$ , so higher-order terms of (4) should be suppressed in the limit  $d \rightarrow \infty$ . Hence, we can perturbatively estimate the expectation value  $V$ . In the leading order, it is approximated by the expectation value in a purely Gaussian theory:

$$V \approx \left\langle e^{it \sum_p S_{j,k}(p) \tilde{x}_p} \right\rangle_2 = \sum_{n=0}^{\infty} \frac{(it)^{2n}}{(2n)!} (2n-1)!! \left[ \sum_{p,q} S_{j,k}(p) S_{j,k}(q) \langle \tilde{x}_p \tilde{x}_q \rangle_2 \right]^n = \exp \left[ -\frac{t^2}{2} \sum_p \frac{S_{j,k}(p) S_{j,k}(-p)}{\beta S_2(p/d)} \right], \quad (7)$$

and we know that

$$\sum_p \frac{S_{j,k}(p) S_{j,k}(-p)}{\beta S_2(p/d)} = \frac{8}{\beta d^2} \sum_p \frac{1}{p} \sin^2 \left( \frac{\pi(j-k)p}{d} \right) \approx \frac{4}{\beta d^2} \log \left| Cd \sin \frac{\pi(j-k)}{d} \right|, \quad (8)$$

which determines a natural time scale of the Gaussian theory  $t \sim d\sqrt{\beta}$ . The leading nonlinear correction to  $V$  is described by a diagram with a single cubic vertex:

$$\begin{aligned} \Delta_3 V &\approx \left\langle id^{5/2} \sum_{p,q=1}^{d-1} S_3 \left( \frac{p+q}{d} \right) \tilde{x}_p \tilde{x}_q \tilde{x}_{-p-q} e^{it \sum_p S_{j,k}(p) \tilde{x}_p} \right\rangle_2 = \\ &= \left\langle id^{5/2} \sum_{p,q} S_3 \left( \frac{p+q}{d} \right) \tilde{x}_p \tilde{x}_q \tilde{x}_{-p-q} \sum_{n=0}^{\infty} \frac{(it)^{2n+1}}{(2n+1)!} \left( \sum_p S_{j,k}(p) \tilde{x}_p \right)^{2n+1} \right\rangle_2 \\ &= t^3 d^{5/2} \sum_{p,q,s,t,u} S_3 \left( \frac{p+q}{d} \right) S_{j,k}(s) S_{j,k}(t) S_{j,k}(u) \langle \tilde{x}_p \tilde{x}_s \rangle_2 \langle \tilde{x}_q \tilde{x}_t \rangle_2 \langle \tilde{x}_{-p-q} \tilde{x}_u \rangle_2 \times \\ &\quad \times \sum_{n=1}^{\infty} \frac{(it)^{2n-2}}{(2n-2)!} (2n-3)!! \left[ \sum_{p,q} S_{j,k}(p) S_{j,k}(q) \langle \tilde{x}_p \tilde{x}_q \rangle_2 \right]^{n-1} \\ &= \frac{t^3 d^{5/2}}{\beta^3} \sum_{p,q} S_3 \left( \frac{p+q}{d} \right) \frac{S_{j,k}(-p) S_{j,k}(-q) S_{j,k}(p+q)}{p(d-p)q(d-q)(p+q)(d-p-q)} \exp \left[ -\frac{t^2}{2} \sum_p \frac{S_{j,k}(p) S_{j,k}(-p)}{\beta S_2(p/d)} \right] \\ &\approx \left( \frac{t}{\beta d} \right)^3 \int_0^1 dx \int_0^1 dy \frac{S_3(x+y) S_{j,k}(-x) S_{j,k}(-y) S_{j,k}(x+y)}{x(1-x)y(1-y)(x+y)(1-x-y)} \exp \left[ -\frac{t^2}{\beta d^2} \int_0^1 dx \frac{S_{j,k}(x) S_{j,k}(-x)}{S_2(x)} \right], \end{aligned} \quad (9)$$

where we took into account that correlation functions of odd number of entries are zero and  $S_2(0) = S_3(0) = 0$ . This expression implies two natural time scales. The first one is the time scale of the Gaussian theory,  $t \sim d\sqrt{\beta}$ , which determines the exponential decay of this correction to the SFF. The second time scale,  $t \sim \beta d$ , comes from the prefactor; this time scale is induced by loop corrections, which add extra fields  $\tilde{x}$  in the correlators and pull down powers of  $1/\beta$ , but do not bring with them extra powers of  $1/d$ . Higher-order nonlinearities and numbers of loops follow the same pattern and become noticeable only for large times  $t \gg \beta d$ . Thus, Gaussian approximation works well enough for smaller times (at least as long as we are concerned with the SFF).

### III. SPECTRAL FORM FACTOR OF THE TOY INTERPOLATING MODEL

For weak perturbations above the permutation circuit limit, the SFF of the toy interpolating model  $U = e^{-igH}S$  exhibits a crystalline-like behavior with damped periodic oscillations. In this section, we estimate the damping factor of these oscillations. We work in the limit  $g \ll 1$  and  $d \gg 1$ . We also assume that matrix  $H$  is drawn from the Gaussian Unitary Ensemble with partition function  $Z = \int dH \exp(-\frac{d}{2} \text{tr}H^2)$ . With such a normalization, eigenvalues of  $H$  fall into the interval  $(-2, 2)$ .

For simplicity, we first assume that the permutation of basis vectors contains a single cycle of maximal length  $d$ , so  $S^d = e^{i\phi}\hat{I}$ . In the unperturbed model  $U = S$ , all eigenvalues are fixed,  $E_n = (2\pi n + \phi)/d$ ,  $n = 0, 1, \dots, d-1$ , and eigenvectors are straightforwardly constructed by following the classical cycle:

$$|E_n\rangle = \frac{1}{\sqrt{d}} \sum_{k=0}^{d-1} e^{-2\pi i k n/d} |\pi^k(0)\rangle = \frac{1}{\sqrt{d}} \sum_{k=0}^{d-1} e^{-2\pi i n \tilde{\pi}(k)/d} |k\rangle, \quad (10)$$

where  $\pi^k(0)$  denotes the  $k$ -th element of the cycle seeded by 0 and  $\tilde{\pi}(k)$  denotes the discrete logarithm, i.e., the distance between elements 0 and  $k$  along the cycle,  $\pi^{\tilde{\pi}(k)}(0) = k$ . The leading correction to eigenvalues,  $E_n \rightarrow E_n + x_n$ , is given by the perturbation theory (since  $x_n \ll 1$ ):

$$e^{iE_n + ix_n} - e^{iE_n} \approx \langle E_n | (e^{-igH} - 1) S | E_n \rangle = e^{iE_n} \langle E_n | (e^{-igH} - 1) | E_n \rangle, \quad (11)$$

hence,

$$x_n \approx -\frac{g}{d} \sum_{a,b=0}^{d-1} H_{ab} e^{2\pi i n [\tilde{\pi}(a) - \tilde{\pi}(b)]/d}. \quad (12)$$

Taking into account that matrices  $H_{a,b}$  are distributed according to the Gaussian unitary ensemble, we can estimate the approximate two-point correlation function of eigenvalues in the limit  $d \rightarrow \infty$ :

$$\begin{aligned} \langle x_m x_n \rangle &\approx \frac{g^2}{d^2} \sum_{a,b,j,k} e^{2\pi i m [\tilde{\pi}(a) - \tilde{\pi}(b)]/d} e^{2\pi i n [\tilde{\pi}(j) - \tilde{\pi}(k)]/d} \langle H_{ab} H_{jk} \rangle \\ &\approx \frac{g^2}{d^3} \sum_{a,b,j,k} e^{2\pi i m [\tilde{\pi}(a) - \tilde{\pi}(b)]/d} e^{2\pi i n [\tilde{\pi}(j) - \tilde{\pi}(k)]/d} \delta_{ak} \delta_{bj} \\ &\approx \frac{g^2}{d^3} \sum_{a,b} e^{2\pi i (m-n)(a-b)} \approx \frac{g^2}{d} \delta_{m,n}, \end{aligned} \quad (13)$$

where we used that  $k \rightarrow \tilde{\pi}(k)$  is a bijection. The momentum-space correlation function is equally flat:

$$\langle \tilde{x}_p \tilde{x}_q \rangle = \frac{1}{d} \sum_{m,n} e^{-2\pi i (pm+qn)/d} \langle x_m x_n \rangle = \frac{g^2}{d} \delta_{p,-q}, \quad (14)$$

which indicates a flat spectrum of quasiparticles in the eigenvalue crystal.

Finally, we take into account that in this approximation, all correlation functions break down into products of

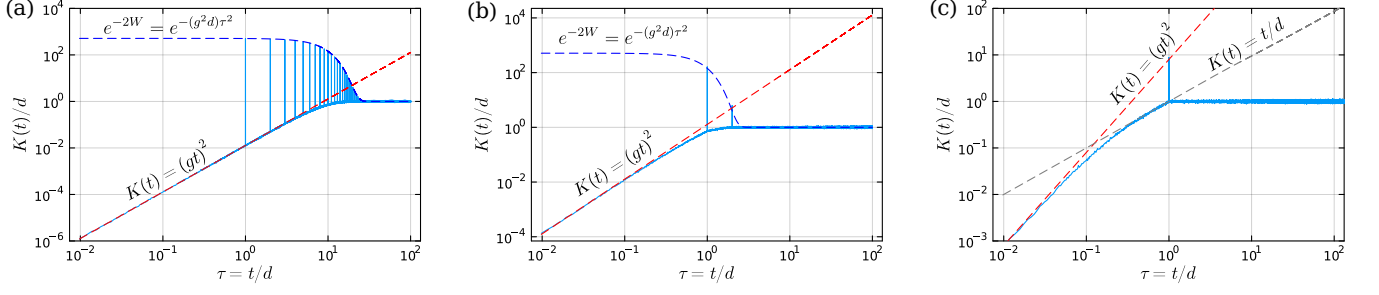


Figure 2. The SFF of the interpolating model  $U = e^{-igH}S$  for  $g = 1/200$  (a),  $g = 1/20$  (b), and  $g = 1/8$  (c). We set  $d = 512$  and average over 1000 samples. Dashed lines denote analytical fits implied by Eq. (15) or circular unitary ensemble universality. Permutation  $S$  contains a single random cycle of length  $d$ .

two-point correlators, which, in turn, decouple due to identity (13). This allows us to estimate the SFF:

$$\begin{aligned}
K(t) &\approx \sum_{j,k} e^{2\pi i(k-j)t/d} \langle e^{it(x_k - x_j)} \rangle = \sum_{j,k} e^{2\pi i(k-j)t/d} \langle e^{itx_k} \rangle \langle e^{-itx_j} \rangle \\
&= d + \sum_{j \neq k} e^{2\pi i(k-j)t/d} \exp\left(-\frac{t^2}{2} \langle x_k x_k \rangle - \frac{t^2}{2} \langle x_j x_j \rangle\right) \\
&= d - d \exp\left(-\frac{g^2 t^2}{d}\right) + \left[\frac{\sin(\pi t)}{\sin(\pi t/d)}\right]^2 \exp\left(-\frac{g^2 t^2}{d}\right).
\end{aligned} \tag{15}$$

So, similarly to the circular beta ensemble, toy interpolating model  $U = e^{-igH}S$  implies periodic SFF with period  $t_H = d$  and Debye-Waller suppression  $e^{-2W} = e^{-(g^2 d)\tau^2}$ :

$$K(t_H \tau) \approx d + e^{-(g^2 d)\tau^2} (d^2 - d), \tag{16}$$

where  $\tau$  is integer. We remind that this approximation is meaningful only when  $g^2 d \ll 1$ . Otherwise, it works only until the Thouless time  $t_{Th} \sim \sqrt{d}/g < t_H$ . At larger times, the SFF approaches the standard ‘‘ramp—plateau’’ form inherent in the circular unitary ensemble, see Fig. 2.

Finally, we extend these results to  $N$  cycles of length  $\{d_1, \dots, d_N\}$ . If the spectrum of  $S$  is not degenerate, all previous arguments work. Hence, similarly to the one-cycle case, we estimate eigenvalue correlations and obtain the same expression for the two-point function (13) and the SFF (15):

$$K(t) \approx d - d \exp\left(-\frac{g^2 t^2}{d}\right) + \left[\sum_{n=1}^N \frac{\sin(\pi t)}{\sin(\pi t/d_n)}\right]^2 \exp\left(-\frac{g^2 t^2}{d}\right). \tag{17}$$

If we remove random phase rotations from  $S$ , i.e., set all  $\phi_k = 0$ , the spectrum of  $S$  becomes degenerate, since all sub-cycles have a common eigenvalue  $E = 0$  (and other common eigenvalues if lengths  $d_1, \dots, d_n$  are not mutually prime). Corrections to such eigenvalues cannot be derived using the non-degenerate perturbation theory, but we can still approximately describe eigenvalue correlations by a theory of non-interacting particles. Assume that  $\bar{x}_n$  are eigenvalues of the correlation matrix  $C_{mn}^{-1} = \langle x_m x_n \rangle$  and introduce the transformation  $x_m = \sum_n X_{mn} \bar{x}_n$ . Then, the SFF is estimated as follows:

$$\begin{aligned}
K(t) &\approx d + \sum_{m \neq n} e^{2\pi i t [m/d(m) - n/d(n)]} \int \prod \bar{x}_k \exp\left[it \sum_p (X_{mp} - X_{np}) \bar{x}_p - \frac{1}{2} \sum_p C_p \bar{x}_p^2\right] \\
&= d + \sum_{m \neq n} e^{2\pi i t [m/d(m) - n/d(n)]} \exp\left[-\frac{t^2}{4} \sum_k \frac{(X_{mk} - X_{nk})^2}{C_k}\right],
\end{aligned} \tag{18}$$

where function  $d(m)$  returns the length of the cycle seeded by  $m$  and  $C_k$  are eigenvalues of  $C_{mn}$ . If number of degenerate eigenvalues is small, then the off-diagonal elements of the correlation matrix  $C_{mn}^{-1}$  exponentially decay, so  $X_{mk} \approx \delta_{mk}$  and  $C_k \approx g^2/d$  for all  $k$ . Hence, in this case, non-degenerate approximation works well. If number

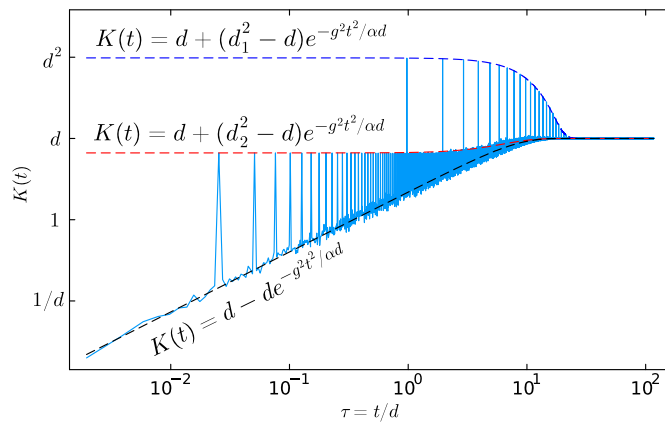


Figure 3. The SFF of the local interpolating model for  $L = 9$  and  $g = 1/500$ . The permutation contains two cycles of length  $d_1 = 499$  and  $d_2 = 13$ . The numerical factor  $\alpha \approx 8$ . We average over  $10^4$  samples. Dashed lines denote analytical fits.

of degenerate eigenvalues grows large, non-degenerate approximation still qualitatively captures the behavior of the SFF, but fails to describe its fine structure. Note, however, that this situation is unlikely if we draw  $S$  randomly, since in this case, it usually has one large cycle  $d_{\max} \sim d$  that dominates the SFF expansion (17) and implies that at least  $\mathcal{O}(d)$  eigenvalues are non-degenerate.

#### IV. LOCAL SHALLOW CIRCUIT FOR THE TOY INTERPOLATING MODEL

Although toy interpolating model  $U = e^{-igH}S$  is convenient for theoretical purposes, it is generally hard to work with matrices  $H$  and  $S$  defined on the entire Hilbert space. So, we suggest an alternative version of this model, in which both  $H$  and  $S$  are converted to depth- $n$  staircase circuits acting on the chain of  $L$  qubits (so,  $d = 2^L$ ):

$$U = \prod_{k=0}^{n-1} \prod_{m=0}^{\lfloor L/n-1 \rfloor} \exp(-igH_{nm+k}) S_{nm+k}. \quad (19)$$

Here,  $H_{nm+k}$  and  $S_{nm+k}$  are  $2^n \times 2^n$  matrices acting in the basis of  $n$  qubits starting from the qubit  $nm+k$ . Similarly to the global model,  $S_{nm+k}$  are classical permutations of computational basis states supplemented with random phase rotations, and  $H_{nm+k}$  are random Hermitian matrices that make evolution (19) inherently non-classical. We assume that local permutations  $S$  are fixed but drawn randomly. Then, we average the SFF of model (19) over the ensemble of matrices  $H$ . If blocks of the circuit are large enough ( $n \geq 3$ ), the length of the largest cycle is comparable to the dimension of the full Hilbert space,  $d_{\max} = \mathcal{O}(2^L)$ . Hence, level statistics of this local model qualitatively reproduces the global model  $U = e^{-igH}S$ , see Fig. 3.